CIMAC CONGRESS 25
ZURICH, MAY 19 – 23, 2025

2025 | 054

Research on Performance Optimization of Methanol Engine Based on the Multi-Model Combined NSGA-II

Controls, Automation, Measurement, Monitoring & Predictive Maintenance

Beidong Zhang, Huazhong University of Science and Technology

Yankun Jiang, Huazhong University of Science and Technology
Jundong Chen, Huazhong University of Science and Technology
Weihong Xu, Huazhong University of Science and Technology

ABSTRACT

Methanol engine represent a crucial direction in internal combustion engine research, with their performance optimization garnering significant attention. The engine itself is a highly coupled, multi-parameter, nonlinear system with interdependent objectives, rendering traditional single-variable or single-objective optimization methods inadequate for meeting its design and optimization requirements. To this end, this paper focuses on a specific methanol engine, utilizing polynomial model, artificial neural network (ANN) model, and GT-Power model, each combined with the NSGA-II algorithm. These methods are employed to optimize and comparatively analyze its operating parameters.

Based on bench tests, the one-dimensional model is calibrated, and the effects of intake timing, ignition timing, and air-fuel ratio (AFR) on engine performance are analyzed to determine the optimization range. With torque and BSFC as optimization objectives, and maximum cylinder pressure, peak pressure rise rate, and exhaust temperature as constraints, three multi-objective optimization methods based on different models are employed to optimize operating parameters such as intake timing, ignition timing, and AFR. The results indicate that the three methods yield varying degrees of optimization effects, with torque increases of 2.39%, 2.22%, and 2.24%, respectively, and average reductions in BSFC of 8.34%, 10.11%, and 10.05%. From the perspectives of optimization effectiveness, efficiency, and applicability, the method based on polynomial model is simple and reliable with relatively high optimization efficiency, though the modeling accuracy is moderate. The method based on the GT-Power model achieves excellent optimization results but incurs high trial and error costs and is approximately 50% less efficient than the other two methods. The method based on the ANN model combines the advantages of good optimization results and high efficiency, with broad applicability, albeit requiring relatively high modeling standards.

1 INTRODUCTION

Methanol, with its wide range of sources, can be extracted or synthesized from various substances such as coal or natural gas, or produced using clean energy through water electrolysis to generate hydrogen combined with CO_2 [1]. It is easy to store and transport, cost-effective, and characterized by a low boiling point and rapid evaporation, which facilitates the formation of mixed gases [2]. With high oxygen content and fast combustion speed, it supports complete combustion, exhibits excellent lean burn properties, and generates fewer harmful emissions, making it a representative "clean alternative fuel" with promising market potential [3]. Developing methanol engines not only reduces the reliance on fossil fuels but also contributes to alleviating environmental pollution [4]. Engine performance has consistently been a key focus in its development [5]. Optimizing the performance of methanol engines can fully unlock their potential and lay a solid foundation for broader promotion and application [6].

Multivariable and multi-objective optimization methods allow simultaneous optimization of multiple parameters and objectives, yielding a series of trade-off solutions that satisfy the given constraints. These methods are particularly well-suited for solving nonlinear system optimization problems like those found in engines, which involve multiple variables and interdependent couplings [7]. With the continuous advancement of new algorithms, such as genetic algorithms, evolutionary strategies, and evolutionary programming, researchers have begun incorporating multi-objective optimization algorithms into engine optimization and design. Consequently, several model-based multi-objective optimization methods for engines have been proposed, which can be categorized into response surface model-based and simulation model-based approaches [8].

The response surface model approximates a complex simulation model with a simpler functional relationship [8]. Two primary methods for multi-objective optimization based on response surface models are polynomial-based models and neural network-based models. For example, Wu [9] and Liu [10] utilized second-order response surface fitting and global optimization algorithms to perform bi-objective optimization on engine power and emissions, as well as torque and fuel consumption rates. Jaliliantabar [10] developed mathematical models linking engine emissions and performance characteristics to factors such as load, speed, EGR rates, and biodiesel fuel rates, optimizing these factors using the NSGA-II algorithm. Etghani [12] used an ANN model to identify optimal biodiesel blends and speed ranges through multi-objective optimization techniques. Similarly, Kakaee [13] utilized a Multi-Layer Perceptron (MLP) network for neural network modeling and combined it with evolutionary algorithms to determine the best engine parameters. This response surface model-based approach to multi-objective optimization offers advantages such as high computational speed and efficiency. However, the optimization effect is greatly affected by the accuracy of the model.

Simulation models are mathematical representations based on computational formulas derived from fluid dynamics, thermodynamics, and other physical principles, offering clearer physical insights compared to response surface models. For instance, Chen [14] integrated the non-dominated sorting genetic algorithm, KIVA-3V, and a master-slave parallel algorithm to optimize injection parameters for improved PCCI combustion, ultimately reducing NOx emissions by 17.34% and soot emissions by 58.23%. Senecal and Reitz [15] utilized the newly developed KIVA-GA global optimization framework to optimize six engine parameters, significantly reducing soot and NOx emissions while improving fuel consumption. Although simulation models are slower in computation compared to response surface models, they offer higher accuracy and clearer physical interpretations. Consequently, simulation model-based multi-objective optimization methods excel in optimization precision and reliability.

Existing research has developed various model-based multi-objective optimization methods for engines, yet no systematic studies have been conducted to comprehensively elucidate their respective strengths and weaknesses—an essential step for the advancement and application of engine multi-objective optimization techniques. Thus, a comparative study of these methods is warranted. This paper takes a 1.3T methanol engine as the research object, with the optimization objectives of maximizing torque and minimizing brake specific fuel consumption (BSFC). The optimization variables include intake timing, ignition timing, and air-fuel ratio (AFR). Using the NSGA-II algorithm, the engine is optimized through three different models: polynomial models, neural network models, and the GT-Power model. Finally, a comprehensive comparison of these three model-based multi-objective optimization methods is conducted to analyze their respective advantages and disadvantages. The findings of this study lay a foundation for further research on multi-objective optimization methods and provide theoretical guidance for their practical application.

2 ENGINE MODELING AND SIMULATION

2.1 Computational model

This study focuses on a 1.3T methanol engine, for which a numerical model is established using GT-Power software. The basic engine parameters are shown in Table 1.

Table 1. Specifications of the engine.

Parameter	Value
Type	In-line, four-stroke
Intake system	Turbocharged Inter-cooling
Cylinder number	4
Injection mode	Multi point injection
Bore×Stroke	75×73.5mm
Displacement	1.3L
Compression ratio	9.5
Number of valves per cylinder	4
Max torque/Speed	195N·m@1600-4000r/min
Rated power/Speed	100kW / 5500r/min

The 1-D GT-Power simulation model, as shown in Figure 1, primarily includes the intake and exhaust systems, turbocharging system, and the cylinder. The main equations used in the modeling process are listed in Table 2.

To ensure that the established engine simulation model accurately predicts engine performance, it is calibrated using data collected from bench tests, including cylinder pressure, torque, and BSFC. Calibration is performed for wide-open throttle conditions at engine speeds of 1000 r/min, 1200 r/min, 1600 r/min, 2000 r/min, 2400 r/min, 2800 r/min, 3200 r/min, 3600 r/min, 4000 r/min, 4400 r/min, 4800 r/min, 5200 r/min, and 5500 r/min. Figure 2 compares the simulated and experimental cylinder pressure curves under operating conditions at 5500 r/min, while Figure 3 compares the simulated and experimental values of torque and BSFC. The results indicate that the maximum error between the simulated and experimental values does not exceed 5%. Therefore, the simulation model is deemed capable of accurately predicting engine performance.

Table 2. Major equations and models.

Item	Content
Basic control equation	Mass conservation equation
	Momentum conservation equation
	Energy conservation equation
Heat transfer model	Woschni heat transfer model
Combustion model	Spark-Ignition Turbulent Flame Combustion Model （SITurb）

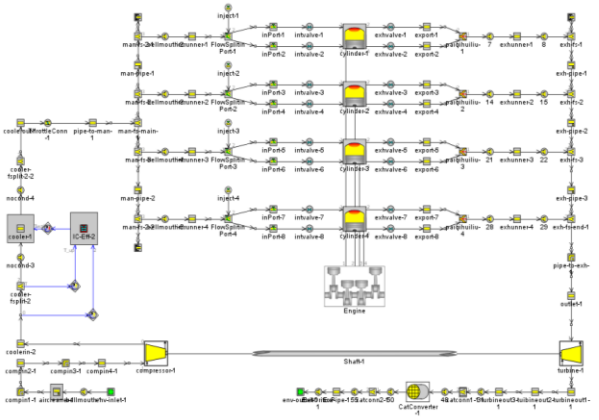

Figure 1. GT-Power model.

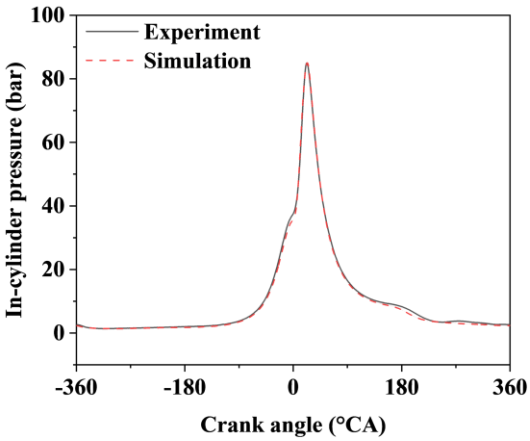

Figure 2. Experimental and simulated in-cylinder pressure (5500rpm).

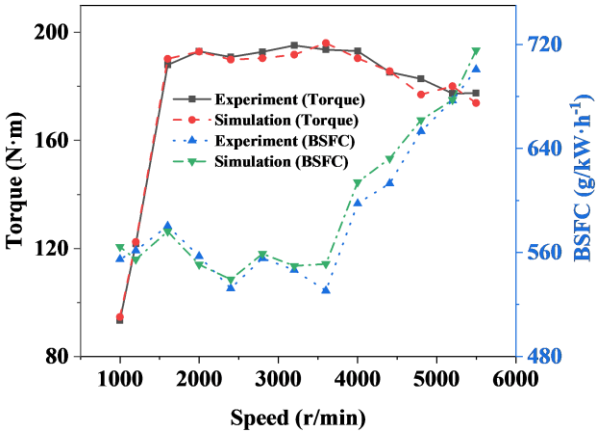

Figure 3. Experimental and simulated external characteristics.

2.2 Simulation results

Intake timing, ignition timing, and AFR are critical parameters that directly determine engine performance [16-18]. Therefore, this section conducts a simulation study to examine the effects of intake timing, ignition timing, and AFR on the

performance of a methanol engine, providing a basis for selecting appropriate optimization ranges.

Under various speed conditions, with the throttle fully open and other operating parameters held constant, only the intake timing is varied to investigate its effects on torque and BSFC. Simulation results for three representative operating conditions—1000 r/min (low speed), 3200 r/min (maximum torque speed), and 5500 r/min (rated speed)—are presented in Figure 4.

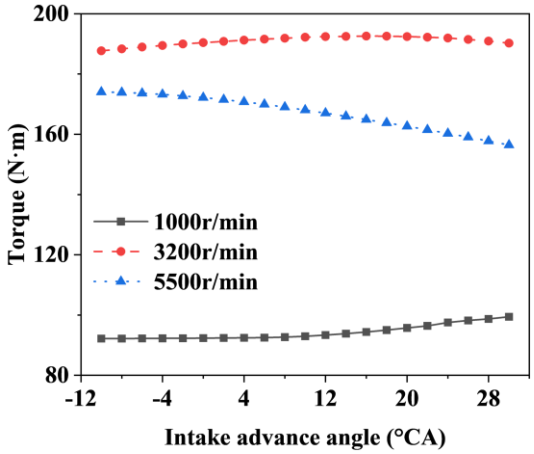

Figure 4(a). Effect of intake timing on engine performance (Torque).

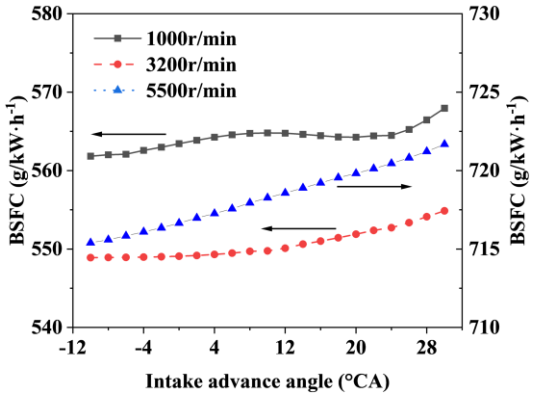

Figure 4(b). Effect of intake timing on engine performance (BSFC).

Under various speed conditions, with the throttle fully open and other operating parameters held constant, only the ignition advance angle (referenced to the compression TDC) is varied to study its effects on engine torque and BSFC. Simulation results for three representative conditions—1000 r/min (low speed), 3200 r/min (maximum torque speed), and 5500 r/min (rated speed)—are presented in Figure 5. Similarly, the simulation results of the effect of AFR on engine performance are shown in Figure 6.

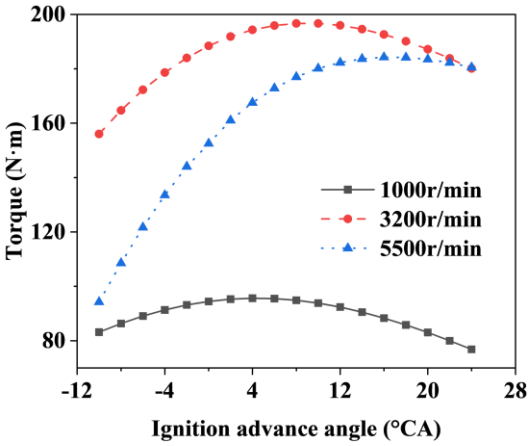

Figure 5(a). Effect of ignition advance angle on engine performance (Torque).

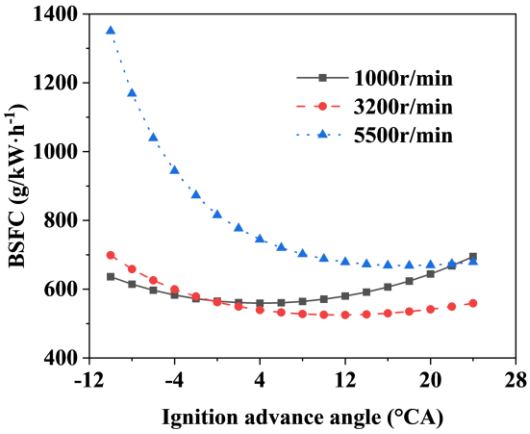

Figure 5(b). Effect of ignition advance angle on engine performance (BSFC).

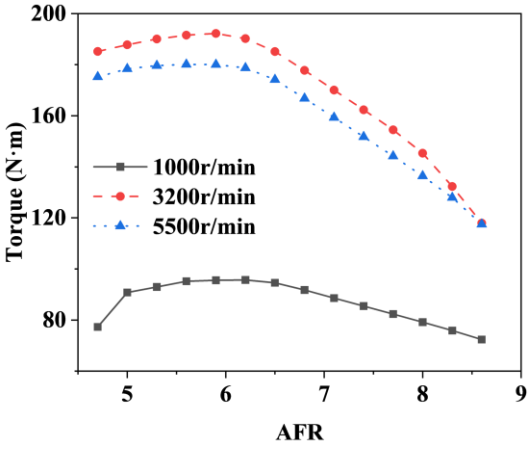

Figure 6(a). Effect of AFR on engine performance (Torque).

Taking into account both power and efficiency, uniform-length optimization ranges for the intake advance angle, ignition advance angle, and AFR were selected under full-load conditions at various engine speeds. These optimization ranges provide

a foundation for subsequent multi-objective engine optimization, as summarized in Table 3.

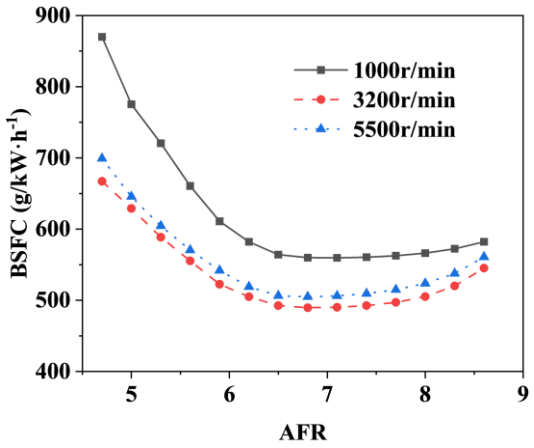

Figure 6(b). Effect of AFR on engine performance (BSFC).

Table 3. Optimization ranges.

Speed (r/min)	Intake advance angle (°CA)	Ignition advance angle (°CA)	AFR
1000	10~30	-7~13	5~8
1200	4~24	-6~14	5~8
1600	0~20	-6~14	5~8
2000	-2~18	-4~16	5~8
2400	1~21	-2~18	5~8
2800	-2~18	-1~19	5~8
3200	3~23	0~20	5~8
3600	-4~16	1~21	5~8
4000	-5~15	4~24	5~8
4400	-8~12	4~24	5~8
4800	-10~10	5~25	5~8
5200	-10~10	6~26	5~8
5500	-10~10	5~25	5~8

3 POLYNOMIAL MODEL COMBINED WITH NSGA-II

3.1 Experimental design

In this study, the DoE (Design of Experiment) optimization toolbox in GT-Power software is utilized for experimental design. Among the methods available, Latin Hypercube Sampling (LHS) is selected due to its ability to achieve comprehensive coverage with minimal experiment, even without an in-depth understanding of the system.

To build a high-accuracy model with as few experimental samples as possible, an analysis is conducted under the condition of a fully open throttle at a speed of 2800 r/min. This analysis explores the impact of sample size on model quality and provides a basis for determining the optimal number of samples.

Research suggests that the relationship between engine performance indicators and adjustment parameters is typically quadratic or cubic [19]. Therefore, a second-order polynomial is initially chosen to establish response models for methanol engine parameters including torque, BSFC, peak cylinder pressure, peak pressure rise rate, and exhaust temperature. Figure 7 illustrates how the quality of these models evolves as the sample size increases from 35 to 1200.

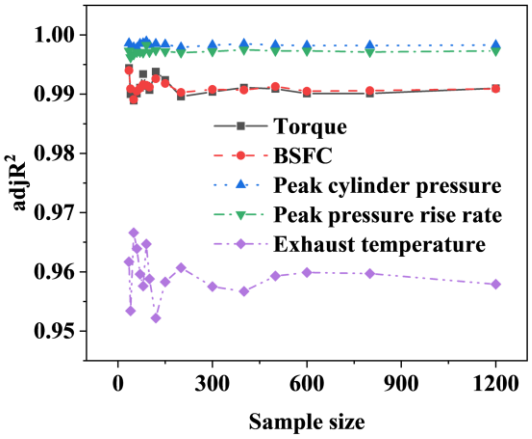

Figure 7(a). Fitting accuracy with sample size.

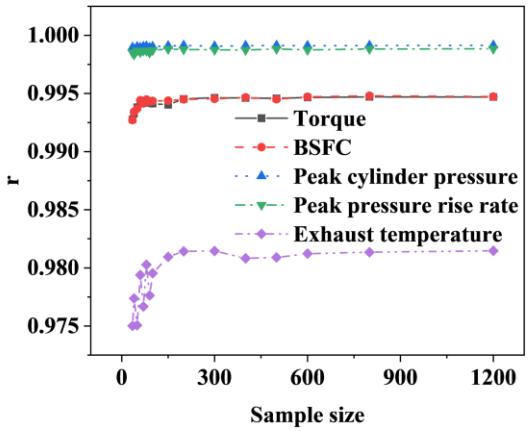

Figure 7(b). Predictive precision with sample size.

As shown in Figure 7, when the sample size reaches 600, the model's fitting accuracy and predictive precision stabilize significantly, with minimal improvement observed as the sample size increases further. To account for variations across operating conditions and ensure adequate robustness, 800 samples are selected for each speed condition to fit the polynomial engine model.

The experimental design includes three variables: intake advance angle, ignition advance angle, and AFR. Their ranges are detailed in Table 3. The

sample points are generated using the LHS algorithm in the DoE toolbox, with the number of variables M=3 and the number of sample points N = 800 for model fitting and N = 200 for validating the model's predictive capability. Figures 8 and 9 illustrate the distribution of the fitting and testing sample points, respectively, under the 2800 r/min condition. The sample points are evenly and reasonably distributed across the experimental space, ensuring comprehensive coverage and reliable model development.

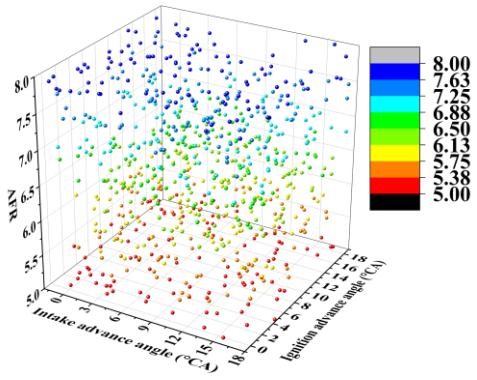

Figure 8. Distribution of fitting sample point.

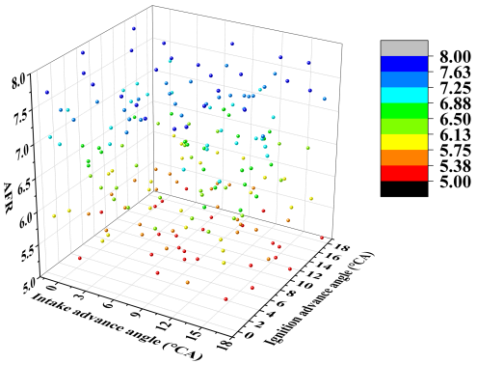

Figure 9. Distribution of testing sample point.

3.2 Construction of polynomial model

When constructing the polynomial model for the engine, it is necessary to determine the polynomial order in advance. The choice of order is typically based on the relationship between engine parameters and performance indicators. To establish a high-precision polynomial model, the quality of the model is analyzed as a function of polynomial order, using the 2800 r/min condition as an example. This analysis provides a reference for selecting the appropriate polynomial order. Table 4 presents the adjR^2, root mean square error (RMSE), and r values of polynomial models with varying orders under the 2800 r/min condition.

As shown in Table 4, with an increase in polynomial order, the adjR^2 and r values steadily rise, while the RMSE values decrease, indicating continuous improvements in model fitting and predictive accuracy. When a fourth-order polynomial model is employed, all adjR^2 values exceed 0.99, RMSE values fall below 4.2, and r values surpass 0.995, demonstrating high model quality. Therefore, a fourth-order polynomial is selected to construct the approximate model for the methanol engine. The mathematical form of the model is expressed as Equation (1):

$$y = \beta_0 + \beta_1 \cdot (InA) + \beta_2 \cdot (SA) + \beta_3 \cdot (AFR) + \beta_4 \cdot (InA) \cdot (SA) + \beta_5 \cdot (InA) \cdot (AFR) + \beta_6 \cdot (SA) \cdot (AFR) + \beta_7 \cdot (InA)^2 + \beta_8 \cdot (SA)^2 + \beta_9 \cdot (AFR)^2 + \beta_{10} \cdot (InA)^3 + \beta_{11} \cdot (SA)^3 + \beta_{12} \cdot (AFR)^3 + \beta_{13} \cdot (InA)^4 + \beta_{14} \cdot (SA)^4 + \beta_{15} \cdot (AFR)^4 \quad (1)$$

Here, y represents the response value, β denotes the polynomial regression coefficients, InA is the intake advance angle, SA is the ignition advance angle, and AFR is the air-fuel ratio.

Table 4. Comparison of the quality of polynomial models of different orders at 2800 r/min.

Index	Response	Order		
		Second	Third	Fourth
adjR2	Torque	0.9906	0.9949	0.9971
	BSFC	0.9913	0.9951	0.9970
	Peak cylinder pressure	0.9983	0.9995	0.9996
	Peak pressure rise rate	0.9974	0.9996	0.9997
	Exhaust temperature	0.9582	0.9635	0.9912
RMSE	Torque	1.2264	0.9055	0.6782
	BSFC	4.0514	3.0433	2.3788
	Peak cylinder pressure	0.7388	0.3866	0.3626
	Peak pressure rise rate	0.0943	0.0367	0.0333
	Exhaust temperature	9.1115	8.5030	4.1560
r	Torque	0.9958	0.9974	0.9986
	BSFC	0.9953	0.9969	0.9983
	Peak cylinder pressure	0.9993	0.9998	0.9998
	Peak pressure rise rate	0.9987	0.9998	0.9998
	Exhaust temperature	0.9800	0.9827	0.9957

Figure 10 presents the adjR^2, RMSE, and r values for five different response models across various engine speed conditions. As shown, all adjR^2 values exceed 0.98, r values are greater than 0.99,

and are very close to 1, while RMSE values remain below 6. These results indicate that the polynomial models exhibit high fitting accuracy and predictive precision.

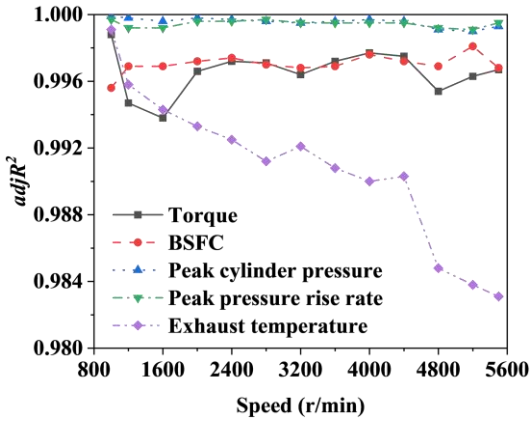

Figure 10(a). adjR^2 of each polynomial model under different working conditions.

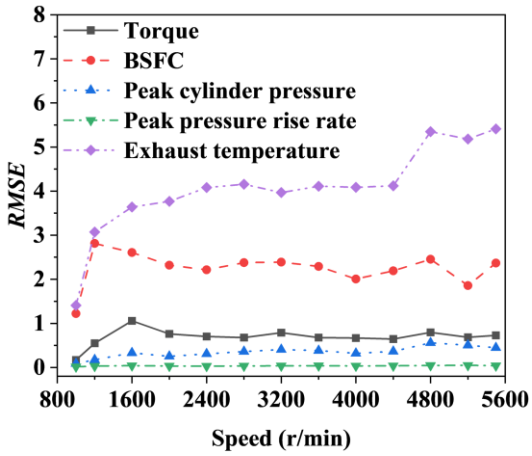

Figure 10(b). RMSE of each polynomial model under different working conditions.

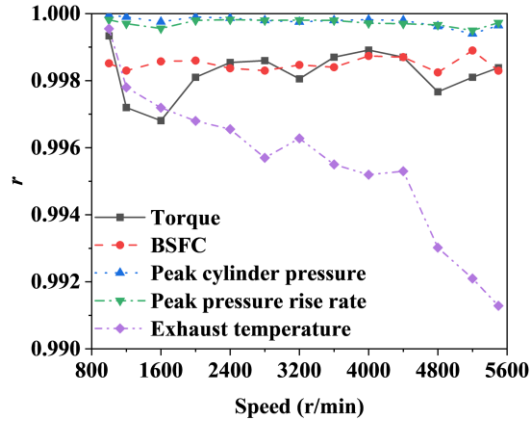

Figure 10(c). r of each polynomial model under different working conditions.

3.3 Optimization results and analysis

Based on the polynomial model constructed in the previous section, the NSGA-II algorithm is employed here for multi-objective optimization of the engine. The optimization aims to maximize torque and minimize BSFC, while incorporating nonlinear constraints such as peak cylinder pressure, maximum pressure rise rate, and exhaust temperature. The mathematical representation of the optimization model can be described as:

Optimization target:

$$\text{Max } Torque(InA, SA, AFR) \quad (2)$$

$$\text{Min } BSFC(InA, SA, AFR) \quad (3)$$

Nonlinear constraints:

$$P_{Max}(InA, SA, AFR) \leq 90 \quad (4)$$

$$Pr_{Max}(InA, SA, AFR) \leq 4 \quad (5)$$

$$T_{em}(InA, SA, AFR) \leq 1150 \quad (6)$$

Here, Torque and BSFC represent torque and brake specific fuel consumption, respectively, serving as the objective functions for the genetic algorithm. P_{Max} denotes the peak cylinder pressure, with a constraint limit of 90 bar [20]. Pr_{Max} represents the maximum cylinder pressure rise rate, which for spark-ignition engines typically falls within the range of 0.20–0.40 MPa/°CA [21]. Hence, a limit of 4 bar/°CA is applied. T_{em} corresponds to the exhaust temperature, expressed in K.

When using the NSGA-II algorithm for optimization, it is generally necessary to handle optimization problems with nonlinear constraints through a constraint-handling technique. Here, the static penalty function method is employed to construct the fitness function, as it is simpler and offers better robustness [22].

To normalize the nonlinear constraints (4) ~ (6), the following steps can be applied:

$$g_1(x) = P_{max}(x) / 90 - 1 \leq 0 \quad (7)$$

$$g_2(x) = Pr_{max}(x) / 4 - 1 \leq 0 \quad (8)$$

$$g_3(x) = T_{em}(x) / 1150 - 1 \leq 0 \quad (9)$$

Among them, x is the optimization variable vector, $x=x(InA, SA, AFR)$.

The fitness function constructed using the static penalty function method can be written as follows:

$$F_1(x) = Torque(x) - R_1\sum_{i=1}^{3} \max[g_i(x),0] \quad (10)$$

$$F_2(x) = BSFC(x) + R_2\sum_{i=1}^{3} \max[g_i(x),0] \quad (11)$$

The penalty factors for the torque and BSFC objective functions are denoted as R_1 and R_2, respectively. Here, R_2 is defined as k times R_1, where k is a factor determined by the ratio of the average BSFC to the average torque in the initial population. After repeated attempts, the parameters for the NSGA-II algorithm were set as follows: population size = 100, number of generations = 100, and penalty factor R_1 = 80. After the optimization process, the pareto optimal set for the two objectives was obtained. The Pareto front is shown in Figure 11.

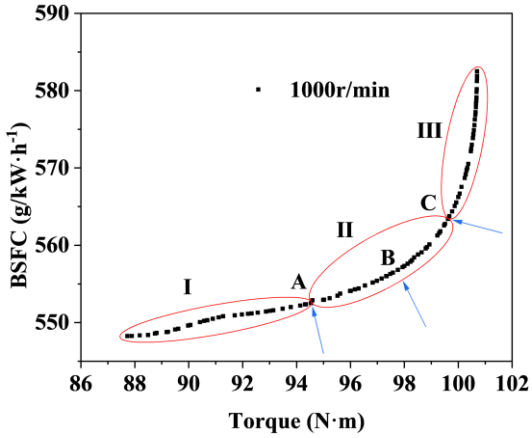

Figure 11(a). Pareto optimal front for each speed condition (1000rpm).

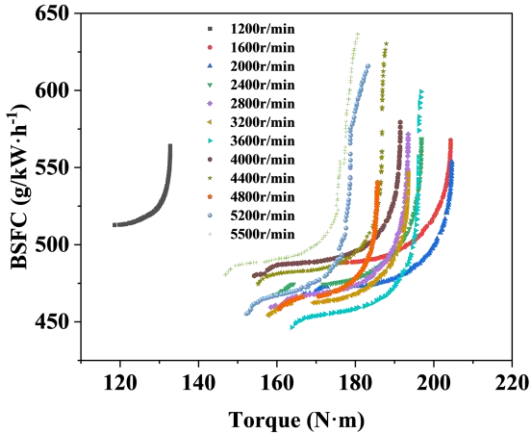

Figure 11(b). Pareto optimal front for each speed condition (1200rpm-5500rpm).

From the pareto optimal front in the figure, it can be observed that there is a trade-off between torque and BSFC. Based on the characteristics of the trade-off between the objectives, the pareto front can be divided into three segments, as illustrated for the 1000 rpm operating condition in Figure 11(a). Segment I is characterized by a slight increase in BSFC, which leads to a significant improvement in torque. Segment III is characterized by a small increase in torque, which results in a sharp rise in BSFC. Segment II is relatively balanced, where significant increases in torque also lead to a noticeable increase in fuel consumption. This segment includes three key points: Point A, located at the endpoint, represents a solution optimized for low fuel consumption. Point C, located at the other endpoint, represents a solution optimized for high torque. Point B, situated in the middle, represents a balanced solution with moderate torque and fuel consumption.

To balance the engine's performance and fuel economy, the first step is to select a feasible solution from the II segment of the Pareto front, ensuring that its torque and BSFC are not worse than the original values. After selecting this feasible solution, the optimized parameter vector is re-entered into GT-Power for simulation, yielding the optimization results. A comparison is made between the original values of engine torque and BSFC, the optimized response prediction values, and the optimized re-simulation values. The results are shown in Figure 12. From this, it can be observed that after optimization, the engine torque is significantly improved at low-speed operating conditions, although the overall increase is modest, with an average improvement of 2.39%. On the other hand, the BSFC decreases substantially across most operating conditions, with an average reduction of 8.34%. Additionally, the response prediction values for torque and BSFC after optimization are very close to the re-simulation values, indicating that the optimization accuracy based on the polynomial model is quite high.

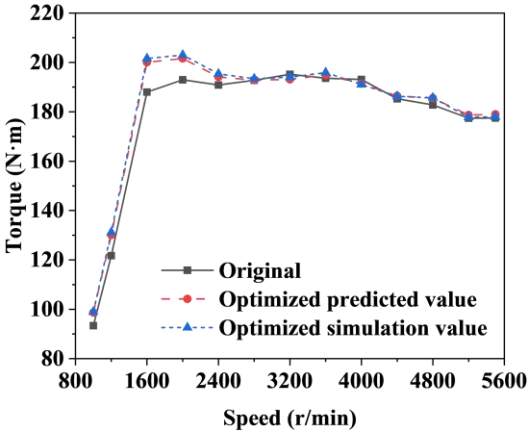

Figure 12(a). Comparison of optimization values with original values (Torque).

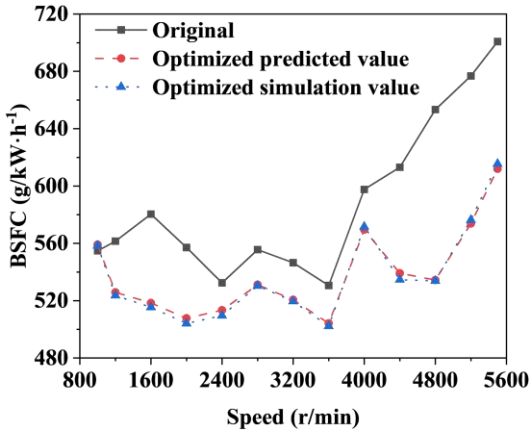

Figure 12(b). Comparison of optimization values with original values (BSFC).

4 ANN MODEL COMBINED WITH NSGA-II

4.1 Construction of ANN model

To ensure consistency in testing methods, this section aligns with the previous content by employing LHS experimental design to select 800 training samples and 200 testing samples for each working condition. The experimental samples are generated using the LHS algorithm from MATLAB's Statistics Toolbox. By calling the X=lhsdesign(n,p) function, an n*p matrix X is returned, where n is the number of samples and p is the number of variables. Here, n and p in the training sample are 800 and 3 respectively, while n and p in the testing sample are 200 and 3 respectively.

Theoretically, a network with a threshold, at least one S-shaped hidden layer, and a linear output layer can approximate any rational function. Generally, increasing the number of hidden layers or nodes within a hidden layer effectively enhances model accuracy but simultaneously complicates the network structure and prolongs training time. Therefore, two- and three-layer BP network models are proposed for engine modeling. The two-layer network is denoted as x-m-y, while the three-layer network is denoted as x-m-n-y, where x represents the number of input layer nodes, m and n represent the number of nodes in the first and second hidden layers, respectively, and y represents the output layer nodes. Taking the working condition at 2800 r/min as an example, the variation in model fitting and prediction accuracy is observed by altering the number of nodes in the hidden layers of the two-layer BP network. The training results, averaged over 10 repeated experiments, are presented in Figure 13.

As shown in Figure 13, the ANN models for torque, peak cylinder pressure, and peak pressure rise rate exhibit high levels of fitting accuracy and prediction precision when using the 3-18-1 network structure. However, the models for BSFC and exhaust temperature perform significantly less effectively. To improve the quality of the ANN models for BSFC and exhaust temperature, a three-layer BP network structure is used. By varying the number of nodes in the two hidden layers, the changes in model quality are observed. The training results for BSFC are illustrated in Figure 14. It is evident that when the BSFC model adopt the 3-16-15-1 network structures, the fitting accuracy and prediction precision are significantly enhanced. Similarly, the exhaust temperature model uses a 3-16-19-1 network structure.

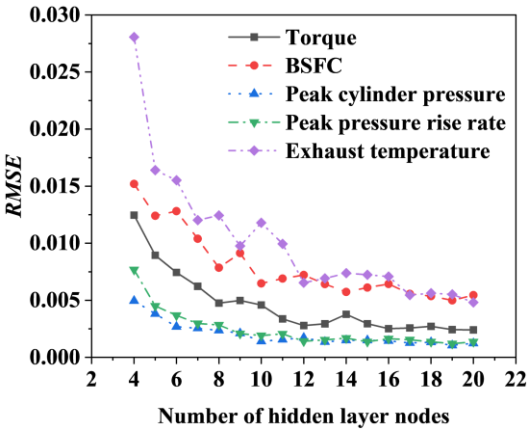

Figure 13(a). Fitting accuracy with the number of hidden layer nodes.

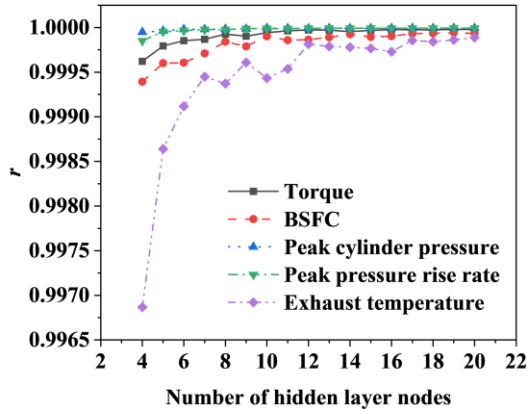

Figure 13(b). Predictive precision with the number of hidden layer nodes.

MATLAB's deep learning toolbox includes various training algorithms based on gradient or jacobian matrices. Using the torque ANN model as test case, 12 different algorithms were employed for training. The basic settings are summarized in Table 5. The training was repeated 10 times and the average value was taken. The results are shown in Table 6.

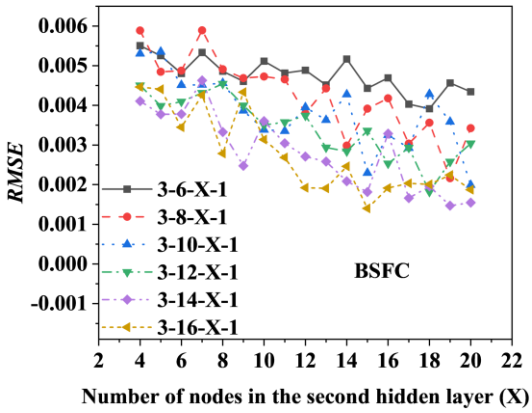

Figure 14(a). Fitting accuracy of BSFC model with the number of hidden layer nodes.

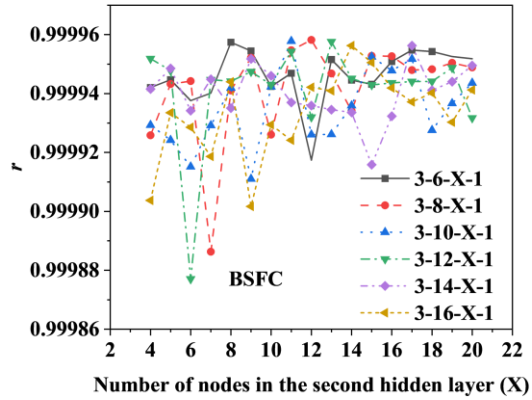

Figure 14(b). Predictive precision of BSFC model with the number of hidden layer nodes.

The training results in Table 6 indicate that the "trainlm" algorithm outperforms the others and is thus selected for training the BP network models.

During the training and validation process, the maximum training generations, target mean squared error, and maximum consecutive validation failures are set to 1000, 0, and 6, respectively. Taking the exhaust temperature ANN model under the 2800 r/min working condition as an example, its training and validation process is illustrated in Figure 15. By the 90th training, the maximum allowable validation failures 6 is reached, satisfying the stopping criterion, and the training is terminated. The optimal validation result, obtained after the 84th training, is retained, with a MSE of 1.4586 x 10-5.

To evaluate the quality of the neural network models, the RMSE of the training set and the r of the testing set are selected as metrics to assess the fitting accuracy and prediction precision. Figure 16 presents the RMSE and r values for the ANN models of torque, BSFC, peak cylinder pressure, peak pressure rise rate, and exhaust temperature across 13 different engine speeds. It can be observed that the RMSE values for all models are below 0.014, and the r values exceed 0.9996. This indicates that the developed ANN models exhibit excellent fitting accuracy and prediction precision, enabling highly accurate predictions of methanol engine performance.

Table 5. Basic settings of BP network.

Content	Parameter
Combination of transfer function	logsig+purelin
Target mean square error (MSE)	0
Maximum number of training generations	10000
Maximum number of consecutive verification failures	20
Training set ratio	0.9
Validation set ratio	0.1

Table 6. Training results of different training algorithms.

Training algorithms	Torque		
	RMSE	r	training duration
trainlm	0.00192	0.99998	2.3s
trainbr	0.00284	0.99997	1.0s
trainbfg	0.00712	0.99988	1.8s
trainrp	0.01091	0.99966	1.3s
trainscg	0.02372	0.99834	0.6s
traincgb	0.01405	0.99938	1.2s
traincgf	0.01581	0.99939	1.1s
traincgp	0.02754	0.99824	0.8s
trainoss	0.02289	0.9987	1.4s
traingdx	0.05023	0.99338	2.2s
traingdm	0.38315	0.55268	9.6s
traingd	0.08965	0.9815	15.6s

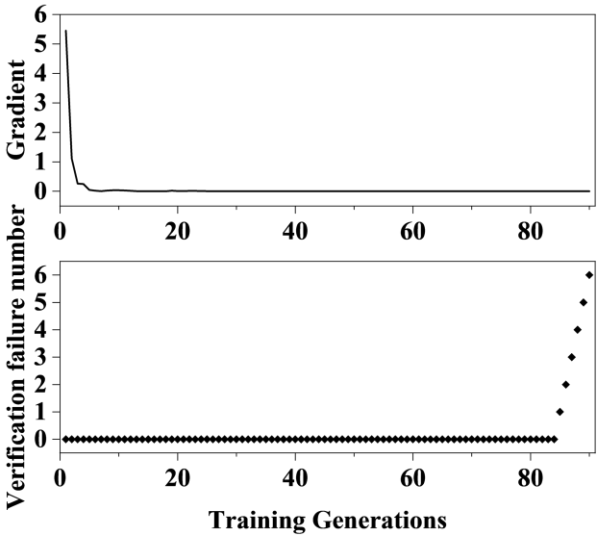

Figure 15. Training status of exhaust temperature ANN model under 2800r/min condition.

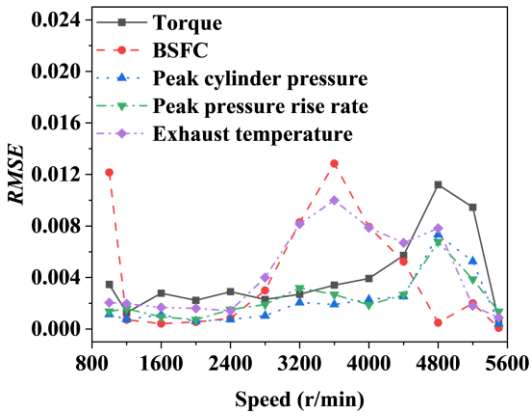

Figure 16(a). RMSE of the ANN models under different working conditions.

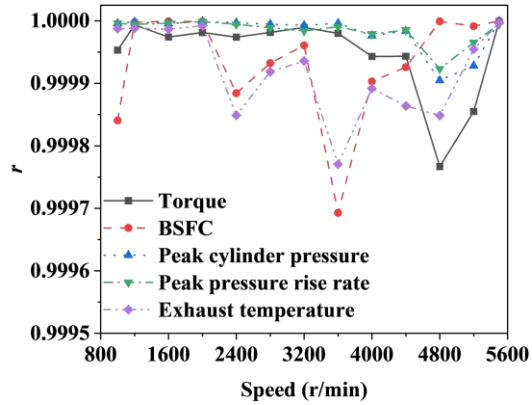

Figure 16(b). r of the ANN models under different working conditions.

4.2 Optimization results and analysis

To achieve optimization of the engine using a combined BP neural network model and the NSGA-II algorithm, an integrated optimization platform was developed. This platform incorporates neural network modeling, NSGA-II algorithm optimization, GT-Power simulation, and data transfer functionalities. The core components of the platform are implemented using MATLAB, which handles neural network modeling and NSGA-II optimization. GT-Power simulations are controlled through Simulink, and the data exchange between MATLAB and GT-Power is facilitated via the Simulink/GT-Power coupling interface. The optimization process based on this platform is illustrated in Figure 17.

During the optimization process, the population size, number of iterations, and penalty factor of the NSGA-II algorithm are consistent with the settings in Chapter 3, set to 100, 100, and 80, respectively. Upon completion of the optimization, a feasible solution is selected from the pareto front for the two objectives under each operating condition. The selected solutions are recalculated using GT-Power to obtain the final optimization results. Figure 18 compares the original values of engine torque and BSFC, the predicted optimized responses, and the recalculated values from the GT-Power simulations.

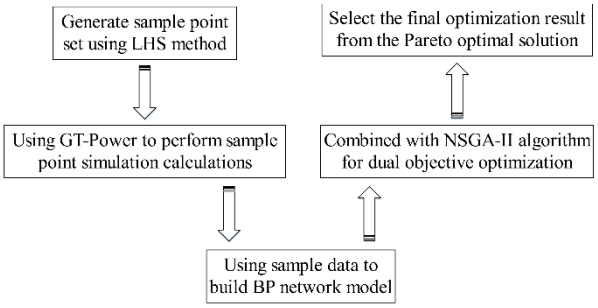

Figure 17. Optimization process of combining ANN model with NSAG-II algorithm.

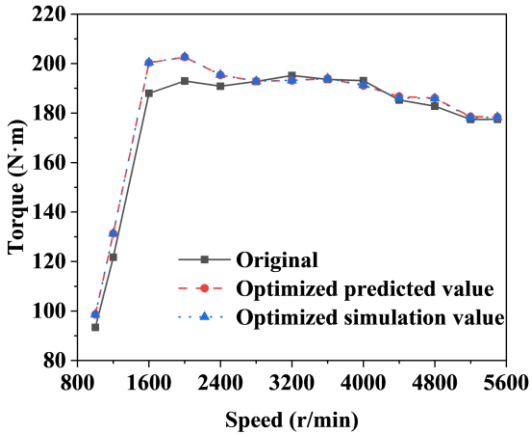

Figure 18(a). Comparison of optimization results based on ANN model with original values (Torque).

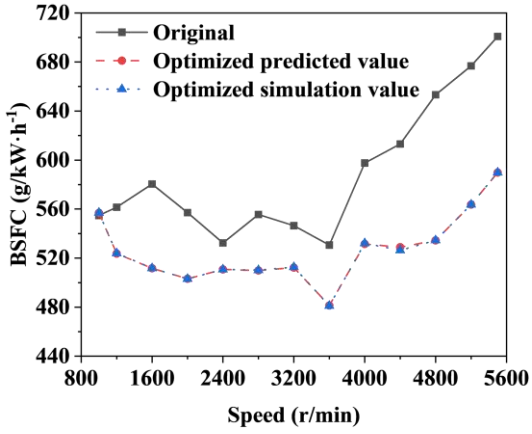

Figure 18(b). Comparison of optimization results based on ANN model with original values (BSFC).

As shown in the figure, after optimization, the engine torque exhibits a noticeable improvement primarily under low-speed operating conditions, with an average increase of 2.22%. Meanwhile, the

BSFC significantly decreases across most operating conditions, with an average reduction of 10.11%. The curves of the predicted optimized responses and the recalculated values from the GT-Power simulations for torque and BSFC are almost identical, demonstrating that the optimization accuracy based on the ANN model is exceptionally high.

5 GT-POWER MODEL COMBINED WITH NSGA-II

5.1 Construction of coupled model

To achieve the combined optimization of the NSGA-II algorithm and the GT-Power model, MATLAB, its Simulink module, and GT-Power are integrated. MATLAB is used to implement the NSGA-II algorithm, Simulink facilitates data exchange, and GT-Power performs simulation calculations. Figure 19 illustrates the coupling-based optimization platform that integrates the NSGA-II algorithm, Simulink, and the GT-Power model.

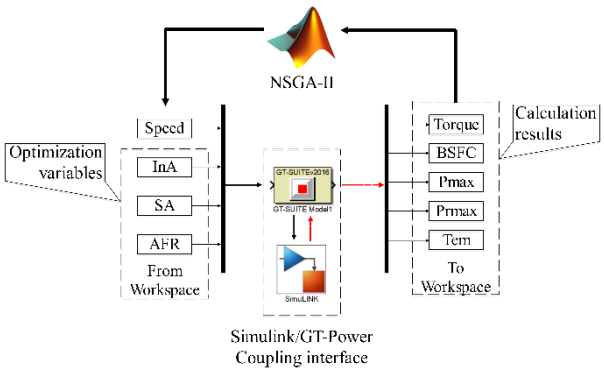

Figure 19. MATLAB/Simulink/GT-Power coupling schematic.

First, the population individuals generated by the NSGA-II algorithm are compiled into a time-continuous step signal. This signal is then input into the GT-Power model for simulation via the Simulink/GT-Power coupling interface. Simultaneously, the simulation results are transmitted back to the MATLAB workspace in real-time. Finally, the simulation result corresponding to the last time point of each step signal is used to calculate the fitness values of the individuals in the NSGA-II algorithm.

5.2 Optimization results and analysis

Using the optimization platform, calculations are performed with the objectives of maximizing torque and minimizing BSFC. At the same time, the InA, SA, and AFR are optimized. The resulting pareto optimal front for torque and BSFC is shown in Figure 20.

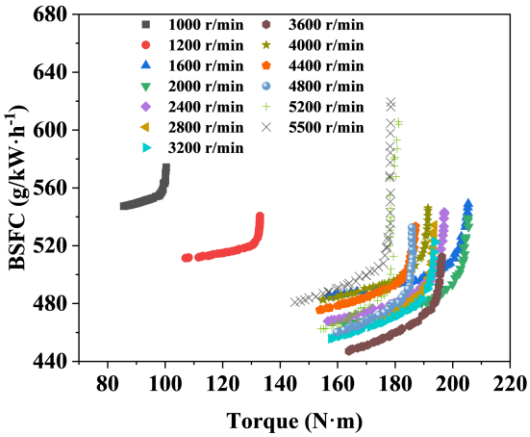

Figure 20. Pareto front for torque and BSFC under different conditions.

After optimization, a feasible solution is selected from the pareto front for the two objectives under each operating condition. Figure 21 compares the optimization results based on the GT-Power model with the original values. It can be seen that different speed ranges exhibit distinct optimization characteristics. In the low-speed range (1000 r/min to 2400 r/min), both engine torque and BSFC show significant improvements. In the mid-speed range (2400 r/min to 4000 r/min), engine torque remains largely unchanged, while the improvement in BSFC is relatively modest. In the high-speed range (4000 r/min to 5500 r/min), engine torque shows a slight increase, and the reduction in BSFC is more pronounced. After optimizing, the engine torque significantly improves only under low-speed conditions, with an average increase of 2.24%. Meanwhile, the BSFC decreases substantially across most operating conditions, with an average reduction of 10.05%. This demonstrates that the optimization method directly coupling the NSGA-II algorithm with the GT-Power model achieves excellent results, significantly enhancing the engine's performance and fuel economy.

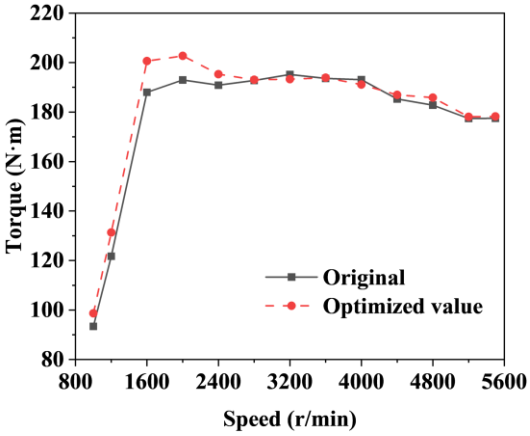

Figure 21(a). Comparison of optimization results with original values (Torque).

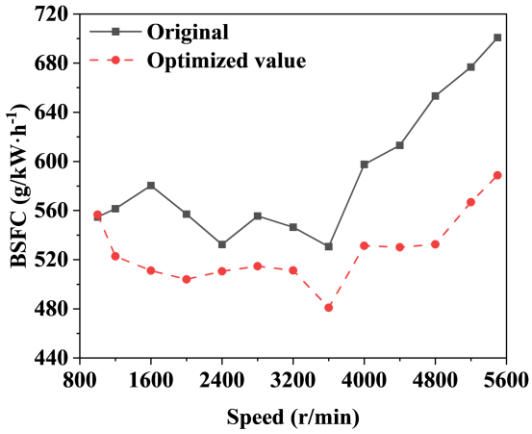

Figure 21(b). Comparison of optimization results with original values (BSFC).

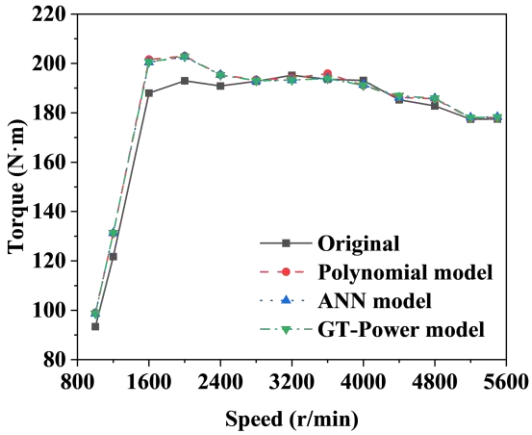

Figure 22(a). Optimization results based on three different models (Torque).

6 COMPARATIVE DISCUSSION OF OPTIMIZATION METHODS

(1) Optimization effects.

The optimization results of the three methods are compared and the results are shown in Figure 22. From Figure 23, it can be observed that the torque differences obtained through the three optimization methods are minimal, with an average deviation of less than 0.2%. However, there is a significant disparity in the BSFC. The BSFC optimized using the ANN model and the GT-Power model shows an average difference of less than 0.1% and is approximately 2% lower, on average, compared to the BSFC optimized using the polynomial model. This indicates that the optimization effects of the ANN and GT-Power models are largely consistent and notably superior to those of the polynomial model.

The GT-Power model can avoid the fitting errors caused by approximating the simulation model as a response model. Therefore, in theory, the optimization results based on the GT-Power model should outperform those based on the ANN model. However, the actual results do not align with this expectation. There are two main reasons for this discrepancy: first, the ANN model exhibits exceptionally high accuracy, almost comparable to that of the GT-Power simulation model; second, to improve the optimization efficiency based on the GT-Power model, the population size and iteration count in the NSAG-II algorithm were set to relatively small values—42 and 36, respectively—much smaller than the values of 100 and 100 used in the optimization based on the ANN model. This led to the pareto optimal solutions obtained using the GT-Power model being less advantageous in terms of both selectivity and convergence.

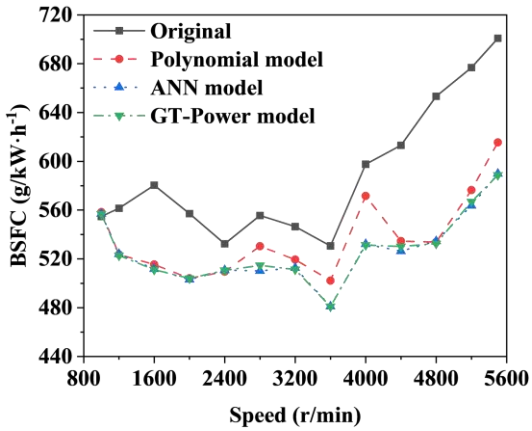

Figure 22(b). Optimization results based on three different models (BSFC).

(2) Optimization efficiency.

The total time consumed by the three optimization methods is primarily dependent on the simulation duration of the GT-Power model. For each operating condition, both response surface-based optimization methods require the simulation of 1,000 sample points, whereas the optimization method based on the GT-Power model requires one initialization and 36 iterations for each of the 42 individuals in the population, amounting to approximately 1,550 simulations. As a result, the total optimization time for the GT-Power model-based method is roughly 1.5 times that of the two response surface model-based methods. All calculations in this study were performed on a quad-core desktop with a 3.5 GHz processor and 8GB of RAM. When converted to full-core computing power, the total optimization time of the three methods are illustrated in Figure 23.

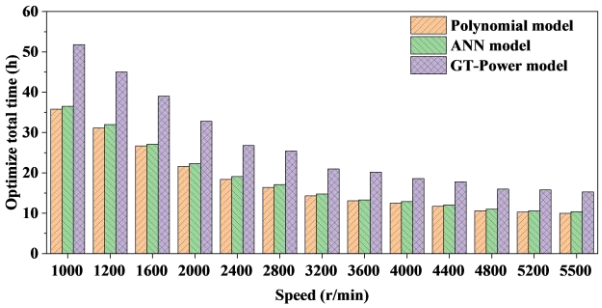

Figure 23. Total optimization time of the three methods.

(3) Trial and error cost.

For the optimization methods based on response surface models, the trial-and-error cost is primarily reflected in the determination of the sample size. In the absence of prior experience, a series of values must be tested to determine an appropriate sample size that ensures the model's accuracy meets the required standards, while also maintaining an acceptable overall optimization efficiency. In contrast, for optimization methods based on the GT-Power model, the trial-and-error cost is reflected in two main aspects. First, the selection of optimization parameters, such as population size, iteration count, and penalty factors, requires multiple trials to determine, with each trial representing a complete optimization computation, thus consuming considerable time. Second, when ideal optimization results are not achieved, re-optimization incurs additional time costs. Unlike the other two methods, which can leverage pre-established response surfaces for rapid optimization, this method necessitates starting from scratch, coupling the NSGA-II algorithm with the GT-Power model for full simulation-based optimization. By comparing the trial-and-error costs of optimization using response surface models versus GT-Power models, it becomes evident that the former is dependent on a single parameter, whereas the latter involves multiple parameters and additional factors. This indicates that the trial-and-error cost for the GT-Power model-based method is generally higher, and it exerts a greater impact on the overall optimization efficiency.

(4) Applicability.

From the above analysis, it can be concluded that the optimization effect of the polynomial model-based method is moderately impacted by the model's accuracy, but it offers high optimization efficiency. The ANN model-based method, with its exceptional accuracy, yields excellent optimization results while also maintaining relatively high efficiency. The GT-Power model-based method, directly coupling the NSGA-II algorithm with the GT-Power model for optimization, provides high computational accuracy and excellent optimization results. However, due to the slower computation speed of the GT-Power model, the optimization efficiency is relatively lower. Based on the characteristics of the three optimization methods, they can be categorized according to the requirements for optimization effect and efficiency in different optimization problems, as shown in Table 7.

Table 7. Classification of the applicability of three model-based optimization methods.

Applicability		Optimization effect requirements	
		Low	High
Optimization effect requirements	Low	Polynomial model ANN model GT-Power model	ANN model GT-Power model
	High	Polynomial model ANN model	ANN model

From the perspective of data source applicability, the NSGA-II algorithm directly coupled with the GT-Power model can only use GT-Power simulation data for engine optimization. In contrast, response surface-based optimization methods can not only utilize simulation data for modeling but, if conditions permit, also incorporate experimental data to construct response models, thereby enhancing optimization accuracy. Thus, response surface-based methods are more adaptable to various data sources, offering greater flexibility.

In the case of optimization with many variables, using the polynomial model-based method may result in insufficient modeling accuracy due to the large sample size required. The GT-Power model-based method, on the other hand, may lead to excessively long optimization times as both population size and iteration count need to increase with the number of variables. The ANN model-based method, however, effectively addresses these issues due to its strong nonlinear mapping capability and high modeling accuracy. Furthermore, its total optimization time primarily depends on sample computation, which increases at a slow rate as the number of variables grows. Therefore, the ANN model-based optimization method is better suited for complex, multivariable engine optimization problems. The main advantages and disadvantages of the three optimization methods are summarized in Table 8.

Table 8. Advantages and disadvantages of the three optimization methods.

<table>
<tr><th>Methods</th><th colspan="2">Advantages</th><th>Disadvantages</th></tr>
<tr><td>Polynomial model combined with NSGA-Ⅱ</td><td rowspan="2">High optimization efficiency, low trial and error cost, strong data acceptance capability, and flexible application</td><td>Simple and reliable modeling</td><td>Average modeling accuracy, inferior optimization effect</td></tr>
<tr><td>ANN model combined with NSGA-Ⅱ</td><td>High modeling accuracy, good optimization effect and wide applicability</td><td>Modeling is relatively complex, and has high requirements on the quality of training data, the design of network structure, and the selection of training parameters.</td></tr>
<tr><td>GT-Power model combined with NSGA-Ⅱ</td><td colspan="2">Accurate and reliable model, good optimization effect</td><td>Low optimization efficiency, high trial and error cost.</td></tr>
</table>

7 CONCLUSIONS

This study focuses on a 1.3T methanol engine, employing three multi-objective optimization methods—polynomial model combined with NSGA-II algorithm, ANN model combined with NSGA-II algorithm, and GT-Power model combined with NSGA-II algorithm—to optimize the engine performance. A comprehensive comparison and analysis of the advantages and disadvantages of these methods were conducted. The main conclusions are as follows:

(1) Multi-objective optimization using the polynomial model combined with the NSGA-II algorithm resulted in a 2.39% average increase in engine torque and an 8.34% average reduction in BSFC.

(2) Multi-objective optimization using the ANN model combined with the NSGA-II algorithm significantly improved the engine's overall performance in terms of power and fuel economy. The torque increased by an average of 2.22%, and the BSFC decreased by an average of 10.11%.

(3) Optimization through coupling the GT-Power model with the NSGA-II algorithm led to an average torque increase of 2.24% and an average reduction of 10.05% in BSFC.

(4) The multi-objective optimization method based on the polynomial model is simple, reliable, and highly efficient, but its optimization results are relatively modest. The GT-Power model-based optimization method yields better results, though its optimization efficiency is lower, and its trial-and-error cost is high. Reducing population size or iteration count to improve efficiency could compromise the optimization outcome. The ANN model-based optimization method, however, strikes a balance between good optimization results and high efficiency, making it highly applicable, although it requires more rigorous modeling.

8 REFERENCES

[1] Shih CF, Zhang T, Li J, et al. 2018. Powering the Future with Liquid Sunshine, *Joule*, 2(10):1925-49.

[2] Tian Z, Wang Y, Zhen X, et al. 2022. The effect of methanol production and application in internal combustion engines on emissions in the context of carbon neutrality: a review, *FUEL*, 320:123902.

[3] Verhelst S, Turner JW, Sileghem L, et al. 2019. Methanol as a fuel for internal combustion engines, *PROGRESS IN ENERGY AND COMBUSTION SCIENCE*, 70:43-88.

[4] Li C, Jia T, Wang H, et al. 2023. Assessing the prospect of deploying green methanol vehicles in China from energy, environmental and economic perspectives, *ENERGY*, 263:125967.

[5] Zhen X, Wang Y. 2015. An overview of methanol as an internal combustion engine fuel, *Renewable and Sustainable Energy Reviews*, 52:477-93.

[6] Svanberg M, Ellis J, Lundgren J, et al. 2018. Renewable methanol as a fuel for the shipping industry, *Renewable and Sustainable Energy Reviews*, 94:1217-28.

[7] Lyantsev OD, Breikin TV, Kulikov GG, et al. 2004. Optimal multi-variable control of gas turbine engines, *INTERNATIONAL JOURNAL OF SYSTEMS SCIENCE*, 35(2):79-86.

[8] Yi-Fang D, Fei L, Wei-Hua Z. 2007. Research on comparative analysis of response surface methods, *JOURNAL OF ENGINEERING DESIGN*, 14(5):359-63.

[9] Chong-Rong WU, Sheng-Li W, Hong-Kun LU. 2019. Research on Multi-Parameter and Multi-Goal Optimization of Diesel Engine Combustion System, *Machinery Design & Manufacture*, (2):13-7.

[10] De-Hui L, Bai-Jun S, Xue-Hua Z. 2016. Multi-Objective Optimization of Intake and Exhaust System of Diesel Engine Based on GT-Power, *Journal of Chongqing Institute of Technology*, 30(7):30-7.

[11] Jaliliantabar F, Ghobadian B, Najafi G, et al. 2019. Multi-objective NSGA-II optimization of a compression ignition engine parameters using biodiesel fuel and exhaust gas recirculation, *ENERGY*, 187:115970.

[12] Etghani MM, Shojaeefard MH, Khalkhali A, et al. 2013. A hybrid method of modified NSGA-II and TOPSIS to optimize performance and emissions of a diesel engine using biodiesel, *APPLIED THERMAL ENGINEERING*, 59(1-2):309-15.

[13] Kakaee A, Rahnama P, Paykani A, et al. 2015. Combining artificial neural network and multi-objective optimization to reduce a heavy-duty diesel engine emissions and fuel consumption, *Journal of Central South University*, 22(11):4235-45.

[14] Chen S, Lin CW, Jia M, et al. 2011. Optimization of Injection Parameters for Diesel PCCI Combustion Based on Genetic Algorithm, *Transactions of Csice*, 29(5):414-21.

[15] Senecal PK, Reitz RD. 2000. Simultaneous Reduction of Engine Emissions and Fuel Consumption Using Genetic Algorithms and Multi-Dimensional Spray and Combustion Modeling, *SAE Transactions*, 109:1378-90.

[16] Krishnamoorthi M, Malayalamurthi R, He Z, et al. 2019. A review on low temperature combustion engines: Performance, combustion and emission characteristics, *Renewable and Sustainable Energy Reviews*, 116:109404.

[17] Xu J, Chang S, Fan X, et al. 2016. Effects of electromagnetic intake valve train on gasoline engine intake charging, *APPLIED THERMAL ENGINEERING*, 96:708-15.

[18] Li J, Gong C, Su Y, et al. 2010. Effect of injection and ignition timings on performance and emissions from a spark-ignition engine fueled with methanol, *FUEL*, 89(12):3919-25.

[19] Zhang DM, Ping T, Chen ZZ. 2016. Optimized Simulation of Performance on Middle Speed Marine Diesel Engine Based on DoE, *Chinese Internal Combustion Engine Engineering*, 37(01):93-7.

[20] Jinliang Z, Yankun J. 2017. Simulation of a Methanol Engine and Selection of Its Compression Ratio, *Internal Combustion Engines*, (4):9-12, 16.

[21] Zhang B, Chen Y, Jiang Y, et al. 2023. Effect of compression ratio and Miller cycle on performance of methanol engine under medium and low loads, *FUEL*, 351:128985.

[22] Michalewicz Z, Schoenauer M. 1996. Evolutionary Algorithms for Constrained Parameter Optimization Problems, *Evolutionary ComputationEvolutionary Computation*, 4(1):1-32.